Nonlinear Dynamics **22:** 205–224, 2000.

Evolution Induced Catastrophe in a Nonlinear Dynamical Model of Material Failure

MENGFEN XIA
Laboratory for Nonlinear Mechanics of Continuous Media, Institute of Mechanics, Chinese Academy of Sciences, Beijing 100080, P.R. China; and Department of Physics, Center for Nonlinear Science, Peking University, Beijing 100871, P.R. China

FUJIU KE
Laboratory for Nonlinear Mechanics of Continuous Media, Institute of Mechanics, Chinese Academy of Sciences, Beijing 100080, P.R. China; and Department of Physics, Center of Nonlinear Science, Beijing University of Aeronautics and Astronautics, Beijing 100083, P.R. China

YUJIE WEI, JIE BAI, and YILONG BAI
Laboratory for Nonlinear Mechanics of Continuous Media, Institute of Mechanics, Chinese Academy of Sciences, Beijing 100080, P.R. China

(Received: 17 June 1998; accepted: 14 May 1999)

Abstract. In order to study the failure of disordered materials, the ensemble evolution of a nonlinear chain model was examined by using a stochastic slice sampling method. The following results were obtained. (1) Sample-specific behavior, i.e. evolutions are different from sample to sample in some cases under the same macroscopic conditions, is observed for various load-sharing rules except in the globally mean field theory. The evolution according to the cluster load-sharing rule, which reflects the interaction between broken clusters, cannot be predicted by a simple criterion from the initial damage pattern and even then is most complicated. (2) A binary failure probability, its transitional region, where globally stable (GS) modes and evolution-induced catastrophic (EIC) modes coexist, and the corresponding scaling laws are fundamental to the failure. There is a sensitive zone in the vicinity of the boundary between the GS and EIC regions in phase space, where a slight stochastic increment in damage can trigger a radical transition from GS to EIC. (3) The distribution of strength is obtained from the binary failure probability. This, like sample-specificity, originates from a trans-scale sensitivity linking meso-scopic and macroscopic phenomena. (4) Strong fluctuations in stress distribution different from that of GS modes may be assumed as a precursor of evolution-induced catastrophe (EIC).

Keywords: Material failure, evolution-induced catastrophe, sample-specificity, binary failure probability.

1. Introduction

Material failure is a problem of scientific and technological importance and has been intensively studied for a long time. However, some fundamental questions still require answering because of the incredible complexity. This complexity comes mainly from the following intrinsic features:

1. Material failure usually results from a nonlinear evolution far from equilibrium.
2. Multi-scale inhomogeneities, especially the collective effects of disordered inhomogeneities on the meso-scopic scale, play a fundamental role in material failure.

This complexity of failure has been noticed by a number of researchers, for example, by Sahimi and Arbabi [1], who wrote:

> In real engineering materials, and in natural rocks, the presence of a large number of flaws with various sizes, shapes, and orientations makes the problem far more complex. Disorder comes into play in many ways during a fracture process. Even small, initially present disorder can be enormously amplified during fracture. This makes fracture a collective phenomenon in which disorder plays a fundamental role. In fact, due to disorder brittle materials generally exhibit large statistical fluctuations in fracture strengths, when nominally identical samples are tested under identical loading. Because of these statistical fluctuations, it is insufficient, and indeed inappropriate, to represent the fracture behavior of a disordered material by only its *average* properties, an idea which is usually used in mean-field approaches: Fluctuations are important and must not be neglected.

In order to clarify the complexity of failure, several lattice or network [1–7], and chain models [8–12] have been developed. A very helpful reference book by Herrmann and Roux [13] summarizes the relevant works until 1990. Various aspects of material failure have been investigated and discussed, such as critical damage fraction, scaling laws, etc.

Among these aspects, one interesting feature has been preliminarily reported which can be sketched by a model called evolution-induced catastrophe (EIC) [4]. The EIC model shows sample-specific behavior, i.e. the macroscopic failure may present very different behavior, sample-to-sample, under the same macroscopic conditions [5]. For instance, it shows a great diversity of EIC thresholds for samples under the same governing macroscopic parameters [12]. There is no direct and simple link between macroscopic and microscopic phenomena for systems far from equilibrium. Moreover, there are rich meso-scopic phenomena which play important roles in material failure. The underlying mechanism of sample-specificity is that the differentiation due to meso-scopic disorder may be strongly amplified during nonlinear evolution from damage accumulation to failure and lead to significantly different macroscopic effects [14].

In most of the previous works, the number of samples is usually limited in comparison with the total number of states in phase space. However, material failure cannot be simply attributed to an equilibrium phase transition, and is severely dependent on microstructures of materials. So, a few examples of computational tests of failure are not enough to draw adequate statistical information. It would be much better to examine the damage evolution to failure by using statistical mechanics, i.e. to examine the evolution of a statistical ensemble.

Ensemble analysis is used to examine the dynamics of a large number of samples. As a first step, it is better to consider simple models with nonlinear dynamics and disorder, for instance, a one-dimensional model. Generally, such a kind of simple model can qualitatively exhibit some important universal behaviors qualitatively. Of course, as the next step, one has to examine the ensemble evolution for two or three-dimensional models to obtain quantitative and more realistic knowledge. Actually, in engineering, one-dimensional fiber models were successfully assumed in the study of composites and proved to be effective (see, for example, [8]).

A preliminary ensemble analysis has been made for short chains based on the examination of all the states in phase space [11]. Obviously, it will become impossible to use this method for long chains owing to the explosively increasing computational complexity. In addition, the commonly used random sampling method cannot reveal the structure of phase space. As we can see later, the structure is extremely important for the study of trans-scale sensitivity. For this sake, a stochastic but interrelated sampling method, called the slice sampling method, is proposed and briefly reported in a short communication [12]. In this paper, a long, one-

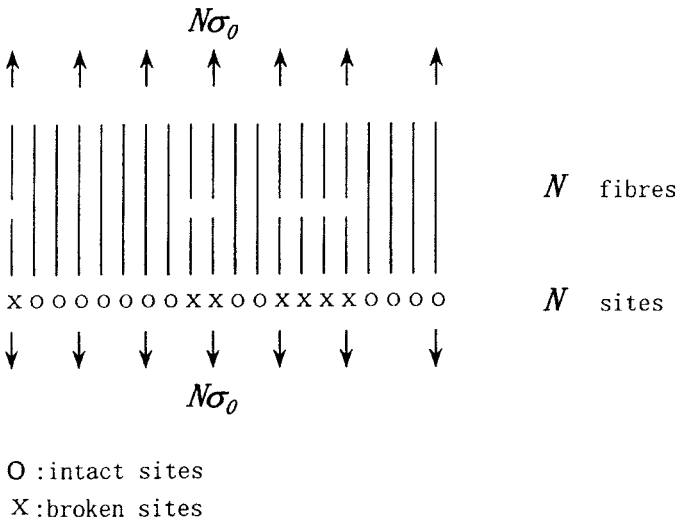

Figure 1. A sketch of a one-dimensional chain model ($N = 20$).

dimensional periodical chain model is adopted as a meso-scopic nonlinear dynamics model of material failure. The slice sampling method is used to study the statistical ensemble evolution. In order to understand the distribution of strength, different from previous works [12, 15], we examined the sample-specific behavior in the binary space of initial damage fraction p_0 and nominal stress σ_0, instead of p_0 only. In this way, we intend to perform a comprehensive and qualitative study of failure and to draw some reliable statistical conclusions on its non-equilibrium essence in disordered materials. Another aim is to find the precursor of failure. These results may be informative for the study brittle failure, like earthquakes, failure of ceramics, etc.

Section 2 gives a brief review of the periodical chain model and slice sampling method. Then, the dynamics of damage evolution and failure probability are introduced in Section 3. Section 4 deals with the sample-specific behavior of failure, the binary failure probability, and the scaling law of size effect. Section 5 considers the diversity of material strength and presents a further discussion on sample-specific behavior. Section 6 examines stress fluctuations in the evolution of EIC modes and the precursor of catastrophe. In Section 7, the sensitive zone in phase space and the statistical description of trans-scales sensitivity are examined. Section 8 is a conclusion.

2. Brief Review of Periodical Chain Model and Slice Sampling Method

In this section we briefly review the periodical chain model [15] and the slice sampling method [12]. Suppose a chain with N sites resembling a bundle of parallel fibers subjected to a tensile load along the fibers, see Figure 1. Such a periodical chain is also called a ring lattice. There are two options in each site, $x_i = 0$ and $x_i = 1$, denoting intact and broken sites, respectively. The meso-scopic damage pattern is denoted by $X = (x_i; i = 1, 2, \ldots, N)$. On the other hand, the macroscopic state of the system can be expressed by a parameter p

$$p = \frac{n}{N} = \sum_{i=1}^{N} \frac{x_i}{N}, \tag{1}$$

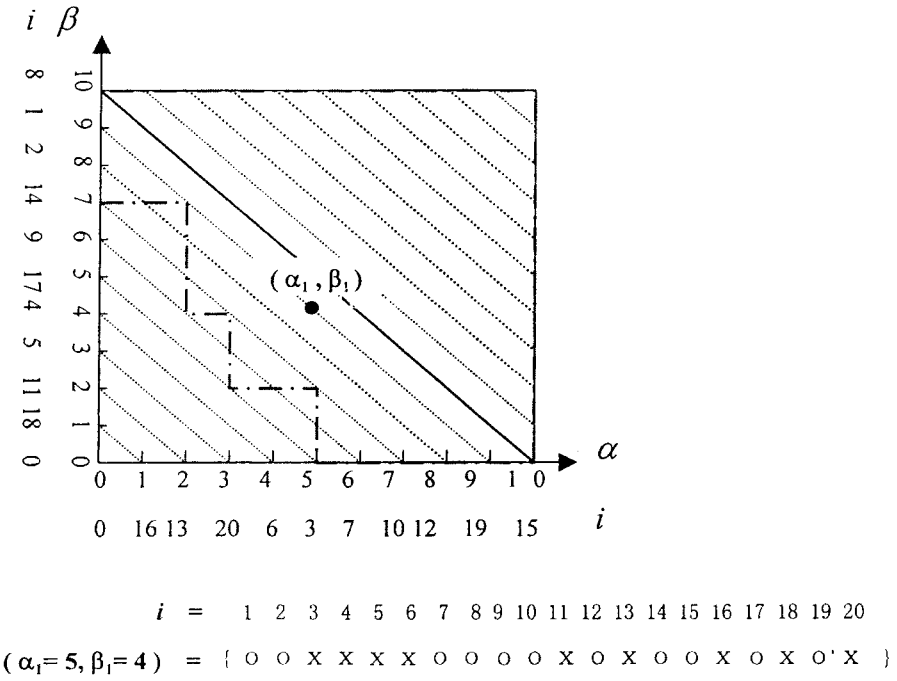

Figure 2. A sketch showing the correspondence between a point on a slice and the damage pattern of a chain ($N = 20$). . . . iso-p-set diagonals, —•— the boundary between GS and EIC based on rule (IV), —- the boundary between GS and EIC based on rule (I).

where p is the damage fraction and n is the total number of broken sites in the chain. The usual approach to the description of all possible damage patterns is to introduce a phase space. A phase point represents the meso-scopic damage pattern of the chain. In terms of the Möbius function and Möbius inversion in number theory, the total number of phase points in phase space, i.e. the total number of possible damage patterns in the chain Ω_N can be exactly calculated [15]. Ω_N rapidly increases with increasing N. For example, $\Omega_N = 52488$ for $N = 20$, $\Omega_N \approx 8.03 \times 10^{57}$ for $N = 200$ and $\Omega_N \approx 5.74 \times 10^{598}$ for $N = 2000$. So, it is clearly impossible to calculate the evolutions of all damage patterns for chains with long periods. To solve the problem, we introduced the slice sampling method [12].

Slices are stochastic two-dimensional sections through phase space, but with interrelated phase points on the slices [16]. Take a two-dimensional coordinate (α, β), where (α and β are integers and $0 \leq \alpha \leq N_1$ and $0 \leq \beta \leq N - N_1$ (N_1 is an arbitrary integer $1 \leq N_1 \leq N$). Let α and β randomly correspond to the individual N sites of the chain (see Figure 2). At a phase point (α_1, β_1), all sites corresponding to $\alpha \leq \alpha_1$ and $\beta \leq \beta_1$ are broken, whereas $\alpha > \alpha_1$ and $\beta > \beta_1$ are intact. Then, a diagonal of the coordinates

$$\alpha + \beta = pN \tag{2}$$

is an iso-p-set, i.e. the damage patterns with the same damage fraction p. Then, the Hamming distance between the two states (α_1, β_1) and (α_2, β_2) on a slice is given by

$$H = \sum_{i=1}^{N} |x_i^1 - x_i^2| = |\alpha_1 - \alpha_2| + |\beta_1 - \beta_2|. \tag{3}$$

So, the states with a shorter Hamming distance H on the slice are closer to each other and all states on the slice are interrelated.

By taking the states on a number of slices as the initial states, we can examine the ensemble evolution of the chain under a given nominal stress σ_0 and a certain load-sharing rule.

3. Dynamics of Damage Evolution and Failure Probability

Now, let us turn to the meso-scopic dynamics of the chain (see Figure 1). The nominal stress σ_0 acting on the chain can be regarded as one of the macroscopic parameters. For simplicity, the strength σ_c of the site is assumed to be the same for all the sites. When the stress σ of a site becomes equal to or greater than the strength σ_c,

$$\sigma \geq \sigma_c, \tag{4}$$

that site will become broken. For a given nominal stress σ_0, the load supported by originally intact but now, due to damage evolution, broken sites is shared by the remaining intact sites. Based on a certain load-sharing rule, the evolution of a damage pattern follows deterministic and irreversible nonlinear dynamics. So, the pattern evolution is determined by the initial pattern, load sharing rule, and macroscopic parameter σ_0/σ_c. According to the final state, evolution modes can be divided into two classes: globally stable (GS) modes and evolution-induced catastrophic (EIC) modes. The ending of the EIC modes is the complete failure state ($p = 1$), whereas the GS modes do not fail and remain globally stable. Obviously, the division of the evolution modes into GS and EIC modes gives an important macroscopic description of the behavior of the system.

In order to cover different types of stress redistribution, we consider the following load-sharing rules (see Figure 3):

(I) Globally mean field rule. The stress is always uniformly shared by all intact sites, i.e., for a chain with damage fraction p, the stress σ is given by

$$\sigma = \frac{\sigma_0}{1-p}. \tag{5}$$

The globally mean field model gives the simplest load-sharing rule without stress fluctuations. The macroscopic strength σ_f of a sample with initial damage fraction p_0 can then be derived from Equation (5) as

$$\sigma_f = (1-p_0)\sigma_c. \tag{6}$$

In addition, for a sample under a given nominal stress σ_0, the failure threshold of damage fraction p_c is given by

$$p_c = 1 - \frac{\sigma_0}{\sigma_c}. \tag{7}$$

Equations (6) and (7) indicate that the failure threshold can be determined uniquely by macroscopic parameters (σ_0, σ_c) or (p_0, σ_c), and then there is a clear-cut boundary between GS and EIC.

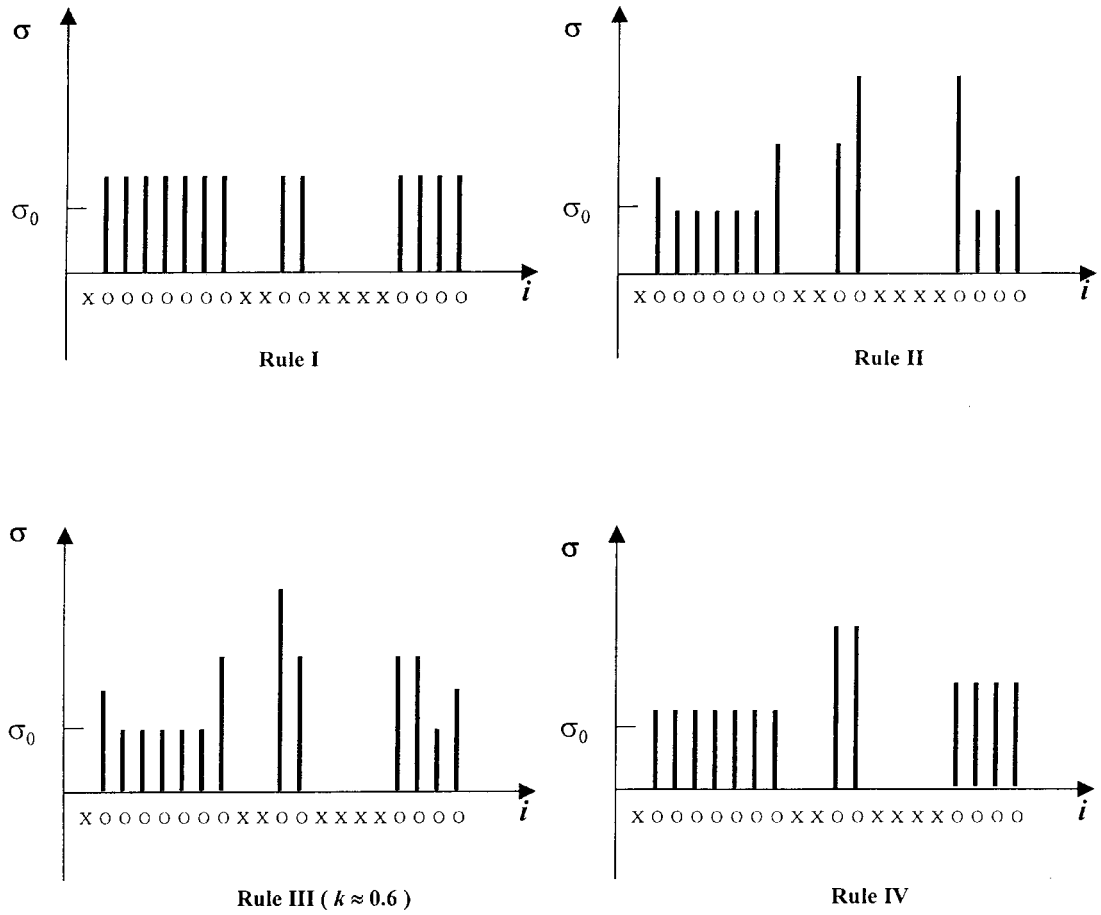

Figure 3. A sketch of four load-sharing rules ($N = 20$).

(II) Stress concentration rule. The nominal stress of a broken cluster will be shared by its two neighboring intact sites.

(III) Influence region rule. There are influence regions on the two sides of a broken cluster, their sizes are proportional to the size of the broken cluster, with a proportional coefficient k. The nominal stress of a broken cluster is shared equally and uniformly by its two influence regions. Once the influence regions of two broken clusters overlap each other, take the mean value to be the stress.

(IV) Cluster load-sharing rule [12]. The nominal stress of a broken cluster is uniformly shared by its two neighboring intact clusters, i.e., a site in an s-intact cluster separating an l- and r-broken cluster supports a stress

$$\sigma = \left(1 + \frac{l+r}{2s}\right)\sigma_0. \tag{8}$$

Then, the corresponding site-breaking condition (4) can be expressed by

$$L = \frac{2s}{l+r} \leq \frac{\sigma_0}{\sigma_c - \sigma_0} = L_c, \tag{9}$$

where L and L_c are the dimensionless and critical dimensionless ligaments, respectively.

According to load-sharing rules (II), (III) or (IV), random stress fluctuations can always occur owing to the random distribution of the broken sites, i.e., owing to the meso-scopic disorder. The stress pattern, determined by damage pattern X, governs the evolution of the damage pattern and evolves with the damage pattern too. So, in these cases, the evolution mode of a system cannot be uniquely determined by macroscopic parameters (damage fraction p and nominal stress σ_0). It is always dependent on the details of the pattern $X = \{x_i\}$, i.e., on the meso-scopic damage pattern. In other words, the system shows sample-specific behavior. Macroscopically, one has to turn to a statistical description.

Now, let us consider an ensemble of samples with the same initial damage fraction p_0 and assume that all the possible damage patterns have the same initial probability. Then, one can examine the ensemble evolution under a given nominal stress σ_0. Especially, one can obtain the probability of the EIC modes, i.e., the failure probability $\Phi_N(p_0, \sigma_0)$, where the subscript N is the period of the chain. $\Phi_N(p_0, \sigma_0)$ gives the most important information about the ensemble evolution to failure. An examination of the evolution of the all-over phase points in phase space has been carried out for the cases of short chains with $N = 20$ and the outcome is shown in Figure 4. One can see that the damage evolutions under rules (II), (III) and (IV) show transitional regions ($0 < \Phi_N < 1$) but rule (I) does not. This means that there is coexistence between GS and EIC modes for given macroscopic p_0 and σ_0. This indicates the complexity of failure, while the mean field model discards the coexistence and is no longer helpful in the issue of failure complexity.

Furthermore, for most cases following rules (II) and (III), the largest initially-broken cluster, independent of all other broken clusters, is usually the most dangerous meso-scopic one. This is due to the fact that the stress concentration at the tip of the broken cluster is irrelevant to other broken clusters, except for the overlapping region in rule (III). In this sense, the failure governed by rules (II) and (III) is still deterministically predictable according to a local criterion for the initial damage pattern, though sample specific. This is what fracture mechanics deal with [17, 18]. So, we shall skip these in this paper.

Finally, rule (IV) reflects the interaction between broken clusters and the evolution depends on the collective effects of the pattern. Under rule (VI), the failure is truly sample-specific and cannot be predicted according to a simple criterion for an initial damage pattern. This is what the nonlinear damage evolution of failure should focus on.

4. Sample-Specific Behavior and Binary Failure Probability

As we have pointed out, the coexistence of GS and EIC modes, i.e. the transitional region of failure probability Φ_N, indicates the sample-specificity and failure complexity. From the angle of meso-scopic damage patterns, this is actually due to the sensitivity of failure to some subtle details of meso-scopic damage patterns, although these patterns have the same macroscopic parameters p_0 and σ_0. In order to reveal the essence of the sample-specific behavior, we must examine large samples. Obviously, the approach to examining all-over phase space is no longer effective for long period chains. We must seek the help of the slice sampling method.

In [12], we have calibrated the method by comparing the results with the exact results obtained by the calculation of the all-over phase points for short chains ($N = 20$ and 30). Here we discuss further the statistical variation of the slice sampling method. For short chains, we can use the exact results obtained from all phase points as the true values. Then, a comparison

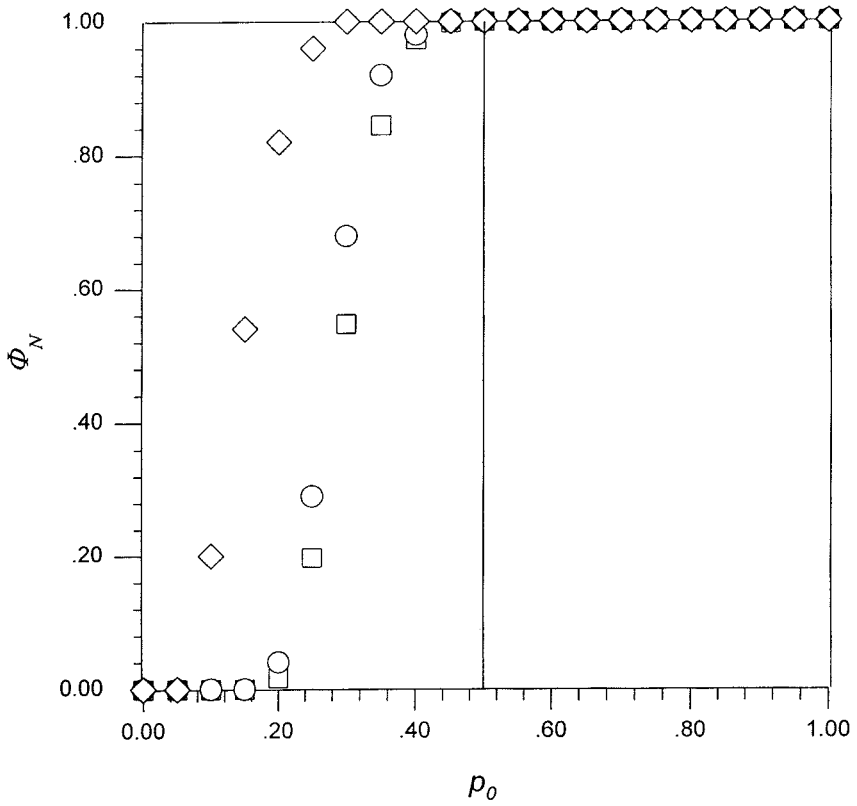

Figure 4. The exact solution of failure probability Φ_N under a given nominal stress ($\sigma_0/\sigma_c = 0.5$) for different load-sharing rules, $N = 20$, — rule (I), ◊ rule (II), ◯ rule (III) ($k = 0.6$), □ rule (IV).

between the results obtained by slice sampling and the true values gives the relative errors. It is found that the errors decrease with the increasing number of slices M. For example, for the chain with $N = 30$, the relative errors of failure probability Φ (at $p_0 = 0.3$ and $\sigma_0/\sigma_c = 0.5$, rule (IV)) are 0.04 for 2000 slices, 0.02 for 10000 slices and 0.0008 for 50000 slices, respectively.

It is impossible to calculate the true values for long chains and then the errors. But by comparing the results from a large number of slices, we can calculate their statistical deviation by taking their mean as approximately the true value. It is found that the deviation decreases with an increasing amount of slices. Figure 5 shows the relative deviations $\Delta\Phi/\bar{\Phi}$ as a function of the amount of slices M ($N = 100$, $p_0 = 0.2$, $\sigma_0/\sigma_c = 0.5$). It is clear that $\Delta\Phi/\bar{\Phi}$ decreases with M, and $\Delta\Phi/\bar{\Phi} < 0.01$ when $M > 20000$, like the errors for short chains.

So the statistical errors and deviations of the slice sampling method decrease with an increasing number of slices. The required precision can be attained by taking sufficient number of slices, for instance, roughly speaking, $(1\sim2) \times 10^4$ slices can give a satisfactory calculation (with (1∼2)% of error or deviation) of the failure probability Φ in practice.

We have briefly reported two features of sample-specific behavior [12]. The first is that the boundary between GS and EIC based on rule (IV) does not coincide with any iso-p-set line (see Figure 2), whereas the mean field theory does. The second are scaling laws of the central position

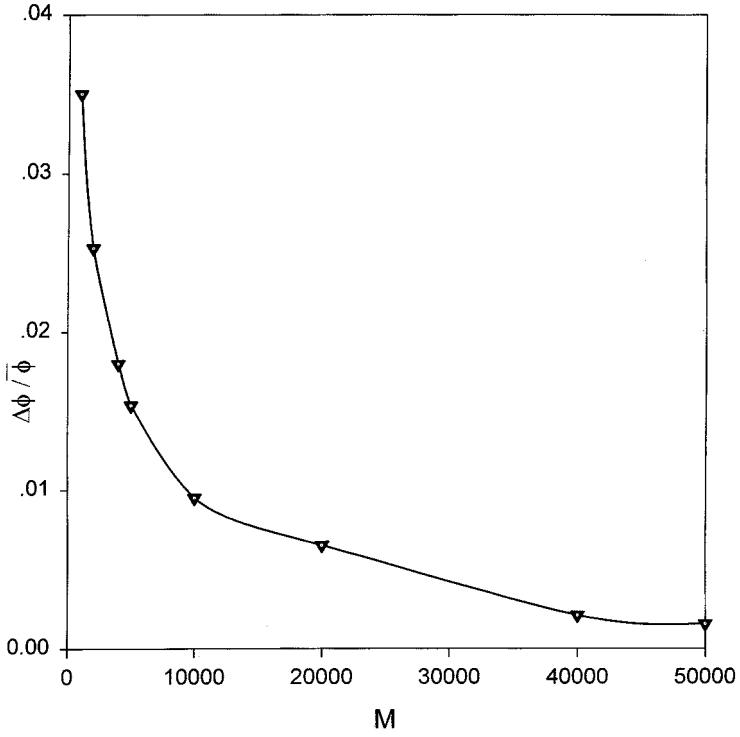

Figure 5. Statistical deviation of the slice sampling method $\Delta\Phi/\bar{\Phi}$, $N = 100$, $p_0 = 0.2$, $\sigma_0/\sigma_c = 0.5$, rule (IV).

$$p_t = \int_0^1 p_0 \frac{\partial \Phi_N}{\partial p_0} \, \mathrm{d}p_0 \tag{10}$$

and the effective width

$$\Delta = \left[\int_0^1 (p_0 - p_t)^2 \frac{\partial \Phi_N}{\partial p_0} \, \mathrm{d}p_0 \right]^{1/2} \tag{11}$$

of the transition region, respectively. Approximately, the scaling laws are $p_t = aN^{-\alpha}$ and $\Delta = bN^{-\beta}$, respectively. The exponents $\alpha = 0.2199$, $\beta = 0.2205$ and the coefficients $a = 0.5454$ and $b = 0.1038$ approximately, for $L_c = 1.0$ in the range of $N \sim (10^1$–$10^3)$. The size span between macroscopic failure (centimeter to meter, typically) and the meso-scopic structure (micrometer, typically) is in the order of 10^4 to 10^6 for a realistic failure of materials. According to the above scaling laws, $\Delta/p_t = 0.1900$ for $N = 10$, $\Delta/p_t = 0.1687$ for $N = 10^6$ [12]. So, sample-specific behavior needs to be taken into account in practical failure.

More importantly, we found that a complete statistical description of sample-specific behavior should be given in two-dimensional parameter space p_0, σ_0, where p_0 is the initial damage fraction and σ_0 is the nominal stress. They are regarded as two macroscopic-governing parameters of a periodical chain. The most important statistical distribution is the binary failure probability $\Phi_N(p_0, \sigma_0)$, instead of the previous $\Phi_N(p_0)$ [12]. Figure 6 shows $\Phi_N(p_0, \sigma_0)$ for $N = 100$ and rule (IV). From Figure 6, one can see that there is a two-dimensional transitional region , where $0 < \Phi_N < 1$, in parameter space $\{p_0, \sigma_0\}$. In this region, GS

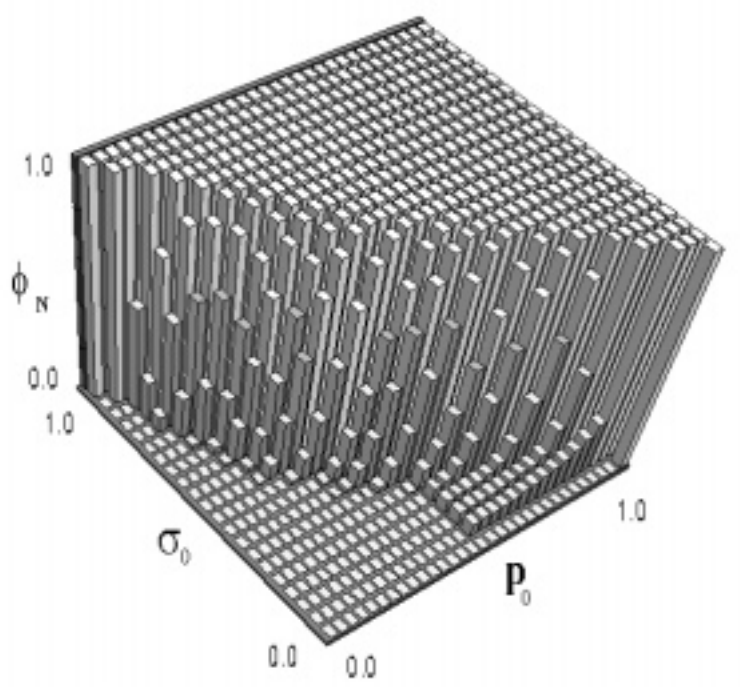

Figure 6. Failure probability $\Phi_N(p_0, \sigma_0)$, for $N = 100$ and rule (IV).

and EIC modes coexist and macroscopic behavior of a system cannot be determined by its macroscopic parameters only.

From probability $\Phi_N(p_0, \sigma_0)$, one can calculate p_t and Δ/p_t as functions of σ_0/σ_c according to Equations (10) and (11). Figure 7 shows these functions for chains with $N = 100$ and rule (IV). Significantly, over the whole range of $0.05 \leq \sigma_0/\sigma_c \leq 0.95$, the relative width of transitional region Δ/p_t, is almost always equal to or greater than the order of 10^{-1} (see Figure 7). This implies that the existence of a transitional region should be taken into account almost always throughout the whole range of nominal stress.

5. Diversity of Macroscopic Strength

One of the most important indications of sample-specific behavior in realistic material failure is that materials generally exhibit large statistical fluctuations in failure strengths under identical macroscopic conditions. Researchers have introduced various empirical statistical distributions of strengths to represent the failure behavior (such as the Weibull distribution).

Obviously, failure probability $\Phi_N(p_0, \sigma_0)$ as a function of σ_0 for a given p_0 gives the cumulative distribution of the failure strength. So the distribution of the failure strength should be derived from $\Phi_N(p_0, \sigma_0)$ by differentiation $W = \partial\Phi_N/\partial\sigma_0$. From Equation (6), we have seen that, for the globally mean field rule, the failure probability Φ is a step function and the distribution of strength is a δ-function. The failure probability of a chain with finite N exhibits a number of jumps in transitional regions because of the stress fluctuations and finite chain size. This causes great difficulties in the calculation of strength distribution. Then, instead, the distribution of failure strength has to be calculated by difference as

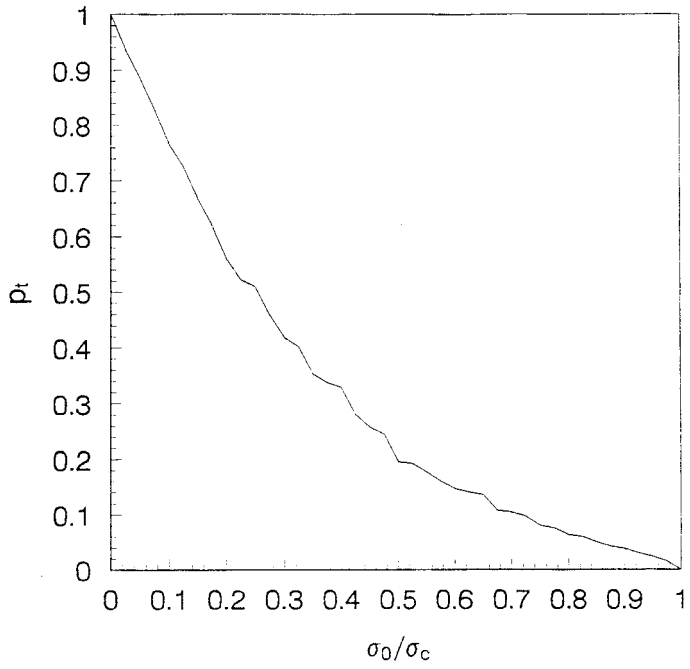

(a)

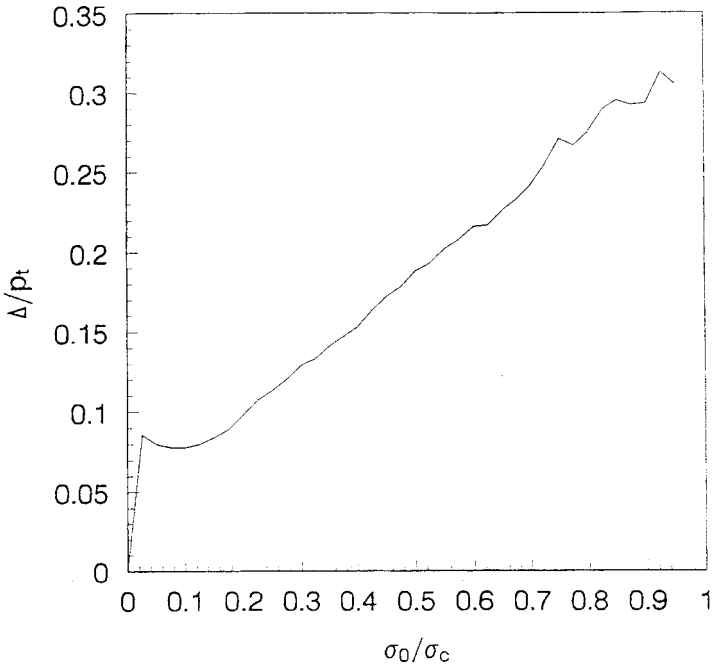

(b)

Figure 7. p_t and Δ as functions of σ_0/σ_c for $N = 100$ and rule (IV): (a) p_t vs. σ_0/σ_c, (b) Δ/p_t vs. σ_0/σ_c.

$$W(\sigma_f, p_0, N) \approx \frac{\Phi_N(p_0, \sigma_f + \Delta\sigma_f) - \Phi_N(p_0, \sigma_f)}{\Delta\sigma_f}, \tag{12}$$

where $\Delta\sigma_f$ is a small but finite increment of strength σ_f.

Figure 8 gives an example of the probability distribution of failure strength W ($N = 600$, $p_0 = 0.2$, rule (IV)). Here the statistical deviation of slice sampling is $\Delta\Phi/\bar{\Phi} \sim 0.01$ for slice amount $M = 50000$ (at $\sigma_0/\sigma_c = 0.4$). Firstly, Φ_N is calculated from 10^5 slices, see Figure 8a. The data of Φ_N are also fitted by a smooth curve $1 - \exp(-b\sigma_f^m)$ (Weibull distribution) with $m = 12.61$ and $b = 10.226$. The standard deviation between the data and the smooth curve is about 0.06, mainly because of the jumps in the data. Figure 8b shows the strength distribution W calculated from the failure probability. The smooth curve is derived from the smooth fitting Weibull distribution in Figure 8a by differentiation. The discrete data demonstrate the results obtained by direct difference of Φ_N.

The average strength of a chain with period N and initial damage fraction p_0 is defined by

$$\bar{\sigma}_f(N, p_0) = \int_0^\infty \sigma_f W(\sigma_f, p_0, N)\, \mathrm{d}\sigma_f \tag{13}$$

and the effective width of the strength distribution is defined as

$$\Delta\sigma_f(N, p_0) = \left[\int_0^\infty (\sigma_f - \bar{\sigma}_f)^2 W(\sigma_f, p_0, N)\, \mathrm{d}\sigma_f\right]^{1/2} \tag{14}$$

by making use of strength distribution W (Equation (12)). Figure 9 shows an example of $\bar{\sigma}_f/\sigma_c$ and $\Delta\sigma_f/\overline{\sigma_f}$ as functions of p_0 ($N = 100$, slice amount $M = 20000$, and the statistical error is less than 0.01, see Figure 5). $\Delta\sigma_f$ is a measurement of the diversity of failure strengths. From Figure 9b, one can see that $\Delta\sigma_f/\bar{\sigma}_f > 10^{-1}$ over a wide range of p_0.

There is an approximate scaling law in the range of ($20 \leq N \leq 2000$) as

$$\Delta\sigma_f/\overline{\sigma_f} = gN^{-\gamma}. \tag{15}$$

For $p_0 = 0.2$, $\gamma = 0.06$ and $g = 0.132$. As the results shown in Figure 9, $\overline{\sigma_f}$ and $\Delta\sigma_f$ are calculated by using Equations (13) and (14), respectively, and the strength distribution W is directly calculated from Φ_N according to Equation (12) by difference. So the precision of $\Delta\sigma_f/\bar{\sigma}_f$ is dominated by the precision of Φ_N. As mentioned before, the statistical deviation of Φ_N is estimated as about 1% (when $M \geq 5 \times 10^4$). The relative deviation of the fitting scaling law (15) is about 10%.

Now, it is still an unbearably time-consuming calculation, even for larger chains with $N > 2 \times 10^3$. So we extrapolate the obtained scaling law (15) to a large size $N = 10^2$–10^6 to have a look of the behavior of $\Delta\sigma_f/\bar{\sigma}_f$. From the extrapolation, $\Delta\sigma_f/\bar{\sigma}_f$ decreases from 0.11 to 0.058 ± 0.005. Such a relative deviation of strength indicates the existence of the strength diversity in the size span $10^2 \leq N \leq 10^6$.

6. Precursor of Catastrophe

Here, we wish to address two questions which we believe are of fundamental importance in the failure of disordered brittle materials. (i) What are the characteristics of an EIC process?

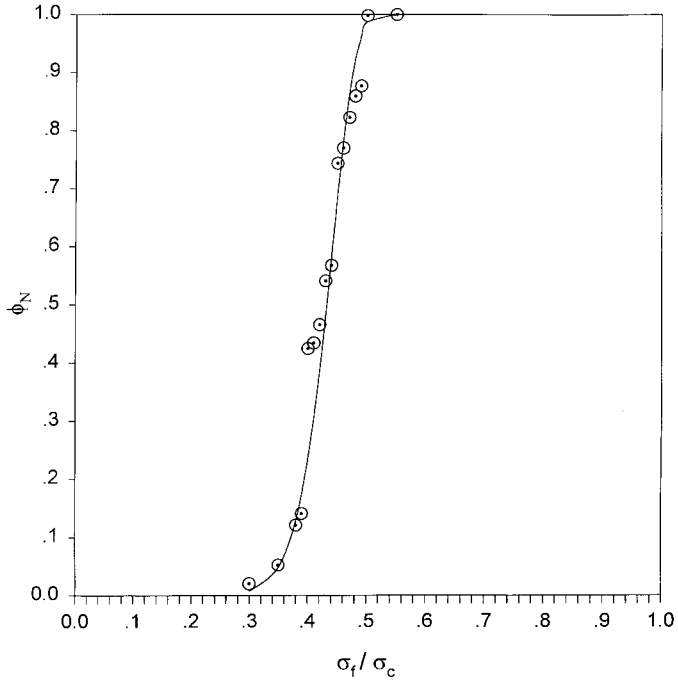

(a)

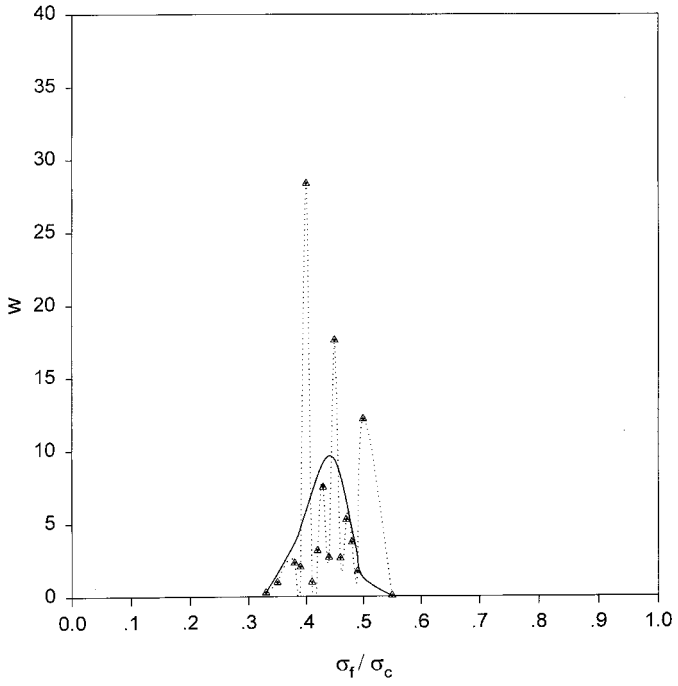

(b)

Figure 8. Probability distribution of failure strength, rule (IV), $p_0 = 0.2$, $N = 600$: (a) cumulative distribution and fitted curve Φ, (b) strength distribution and fitted curve W.

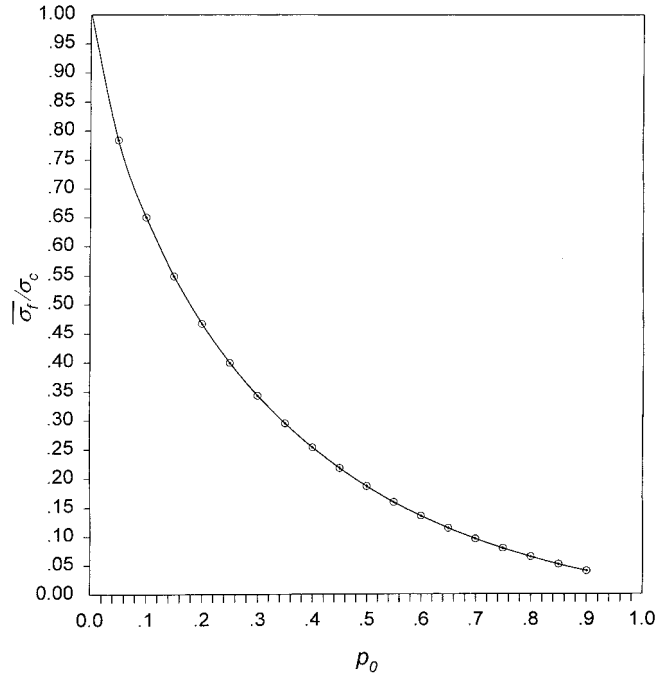

(a)

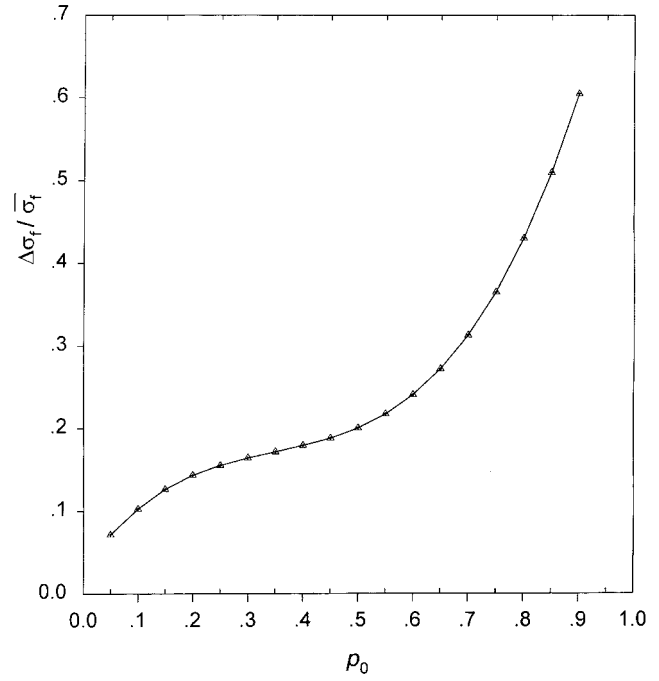

(b)

Figure 9. The dependence of $\bar{\sigma}_f/\sigma_c$ and $\Delta\sigma_f/\bar{\sigma}_f$ on the initial damage fraction p_0, $N = 100$, rule (IV). (a) $\bar{\sigma}_f/\sigma_c$ vs p_0 and fitted curve, (b) $\Delta\sigma_f/\bar{\sigma}_f$ vs. p_0 and fitted curve.

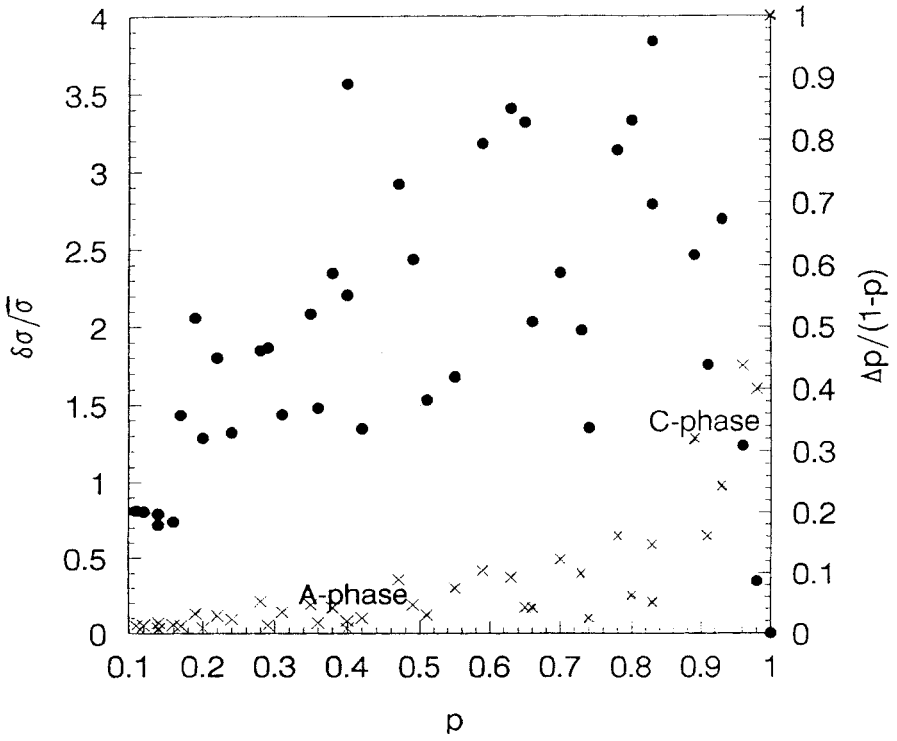

Figure 10. Evolution of EIC mode and stress fluctuations ($N = 1000$, $\sigma_0/\sigma_c = 0.5$, rule (IV), and initial damage fraction $p_0 = 0.1$). Around $p \sim$ (0.8–0.85), the relative damage rate ($\times$) increases rapidly and the relative stress fluctuations ($\bullet$) attain maximum: $\times$ the relative damage rate $\Delta p/(1-p)$, $\bullet$ the relative stress fluctuations $\delta\sigma/\bar{\sigma}$, $\delta\sigma$ is the standard deviation of the stress distribution.

(ii) What is the precursor of a catastrophe? If such a precursor does exist, it may help us to predict catastrophes, like earthquake. Let us make a comparison between the EIC and GS modes. Choose macroscopic parameters (p_0, σ_0) in the transitional region, where EIC and GS modes coexist. The damage fraction p is a variable, which varies from the initial value p_0 to a finite one p_f, $p_f < 1$ for GS modes and $p_f = 1$ for EIC modes. The relative damage 'rate' can be described by $\Delta p/(1-p)$, where Δp is the increment of p in a 'time step', i.e., the increment of p induced by a stress redistribution. Firstly, we select an example of the EIC mode to examine its variation in the relative damage rate with increasing damage fraction p, which is shown in Figure 10 ($N = 1000$, $p_0 = 0.1$, $\sigma_0/\sigma_c = 0.5$ rule (IV)). The variable p may be regarded as an equivalent time, though it is not a linear function of real time.

It is found that the EIC mode does show a transition from slow to rapid growth in the relative damage rate. The major part of the life time is dominated by a slow regime, where the damage accumulates slowly. So we call the slow regime the A-phase. Within a narrow region in the vicinity of $p \sim 0.85$, the damage evolution transits to a regime with a very rapidly increasing relative damage rate and then catastrophe occurs. This latter regime will be called the C-phase. The simulation for a number of samples shows that the transition from the A-phase to the C-phase is a common characteristic of EIC modes. These numerical results qualitatively coincide with observations of brittle materials failure.

Then, what is the precursor of a catastrophe? According to the mean field approximation, failure should punctually occurs at the critical point p_c given by Equation (7), and the samples

shown in Figure 10 can never go to failure because of $p_0 < p_c$. Therefore, the failure observed in cases $p_0 < p_c$ should be attributed to stress fluctuations resulting from a disordered distribution of damages. By assuming $P(\sigma)$ be the probability distribution of stress, the stress fluctuations in a system can be measured by relative deviation of stress $\delta\sigma/\bar{\sigma}$, where

$$\delta\sigma = \left[\int_0^\infty (\sigma - \bar{\sigma})^2 P(\sigma)\,\mathrm{d}\sigma\right]^{1/2} \tag{16}$$

and

$$\bar{\sigma} = \int_0^\infty \sigma P(\sigma)\,\mathrm{d}\sigma \tag{17}$$

are the standard deviation of stress and the averaging stress, respectively, where $P(\sigma)$ is the distribution of stress σ. From Figure 10, we can see that the stress fluctuations keep at a relatively low level during the initial stage of the A-phase. However, just before the transition from the A-phase to the C-phase, obvious stress fluctuations emerge (the strong fluctuations occur in the range $0.4 \leq p \leq 0.8$ and the maximum level of fluctuations occurs at $p = 0.8$). The catastrophe occurs generally following the peak of relative stress fluctuations. In this sense, the strong stress fluctuations could be considered as a precursor of the transition to catastrophe. The enhancement of stress fluctuations can be attributed to the amplifying effect of disorder during nonlinear evolution.

Now, we compare the stress fluctuations of EIC modes with these of the GS modes for given macroscopic parameters (p_0, σ_0). It is found that the level of stress fluctuations can be considered as a mark of distinct GS and EIC modes. Let θ be the maximum of $\delta\sigma$ in the whole evolution process of a sample. Clearly, the values of θ are different for samples even with the same initial damage fraction. Let $\pi(\theta)$ be the distribution function of θ for a group of samples with the same initial damage fraction. Figure 11 shows that $\pi(\theta)$ is a double-peak distribution, the peak at low θ is related to GS modes and that at high θ is related to EIC modes. The positions of peaks $\hat{\theta}_{\mathrm{GS}}$ and $\hat{\theta}_{\mathrm{EIC}}$ are separated far away at about two orders ($\hat{\theta}_{\mathrm{EIC}}/\hat{\theta}_{\mathrm{GS}} \sim 60$).

To conclude, provided an alert value of maximum stress fluctuation θ is prescribed, one can readily detect an EIC mode before a catastrophe occurs. The alert value can be set in a broad range, for example, between 2 and 30 in the example shown in Figure 11. The greater the alert value is set, the closer to catastrophe the prediction is. During damage evolution, if we can monitor the level of the stress fluctuations and find some level going beyond the alert level, we could say that the catastrophe would appear. Unfortunately, just how close to the catastrophe remains unknown in this approach.

7. Trans-Scale Sensitivity and Transition Probability

The underlying mechanism of the above-discussed sample-specific behavior is the sensitivity of the macroscopic failure to the details of the meso-scopic damage pattern. This is a trans-scale sensitivity linking meso-scopic and macroscopic phenomena. The difference in the meso-scopic pattern can be measured by their Hamming distance defined by Equation (3). For example, two phase points with a Hamming distance of $H = 1$ are defined as neighboring

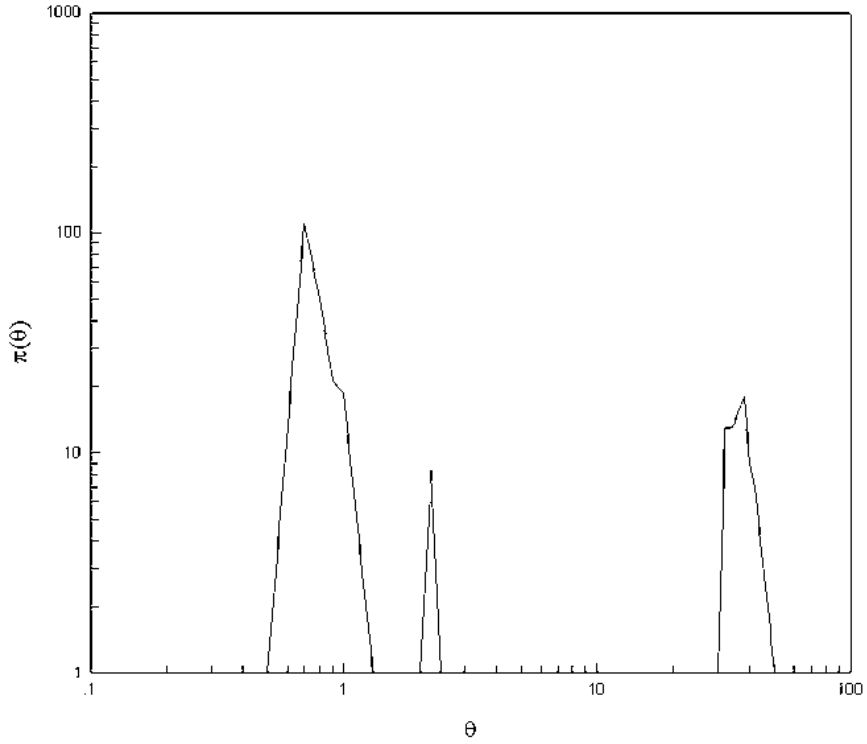

Figure 11. Distribution function $\pi(\theta)$, $N = 1000$, $p_0 = 0.1$, $\sigma_0/\sigma_c = 0.5$, rule (IV). The double peaks indicates the distinction between GS and EIC.

states. According to the evolution modes, the phase space can be divided into a GS region and a EIC region. Actually, the trans-scale sensitivity originates from a sensitive zone in the vicinity of the boundary between the GS and EIC regions (see figure 1 in [12]). In the sensitive zone, a slight change in the meso-scopic pattern can trigger a significant macroscopic consequence, which may especially result in the transition from GS modes to EIC modes.

Now we can give a definition of a sensitive zone. The GS region of the phase space can be divided into two zones. The first zone is called the insensitive zone, where all the neighboring states of a state in the zone are GS states. The second is called the sensitive zone of the GS region, where a GS state has at least one EIC state as its neighboring state. The phase space for a periodical chain with period N is an N-dimensional space and a state has N neighboring states in different directions. For a state with damage fraction p, there are $N(1-p)$ neighboring states along a p-increasing direction. Let m be the number of neighboring EIC states for a GS state. It is obvious that $m = 0$ indicates the GS states in the insensitive zone and $1 \leq m \leq N(1-p)$ indicates the GS states in sensitive zone. Define

$$\mu = \frac{m}{N(1-p)}, \tag{18}$$

where μ gives a measurement of sensitivity for a GS state. In fact, by changing an intact site to be broken stochastically in a GS state, the probability of transition from GS to EIC is given by the value of μ of this state. Figure 12 shows the sensitivity μ on a slice. The value of μ cannot be determined by macroscopic parameters p_0 and σ_0 only. It represents sample-specific

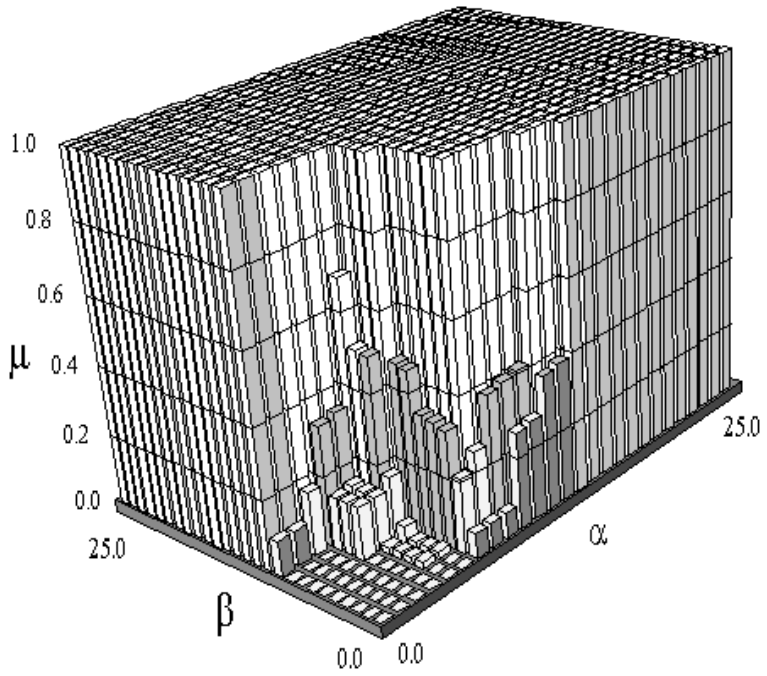

Figure 12. Sensitivity μ of GS states on a slice, $N = 50$, $N_1 = 25$ and $\sigma_0/\sigma_c = 0.5$, rule (IV).

behavior too. Clearly, the sensitive zone spreads all over the transitional region, because the latter is a coexisting region of GS and EIC.

Now we turn to the implication of the sensitive zone in material failure. Up to now, the discussed evolution rules are irreversible deterministic dynamics. More generally, we can consider a system where deterministic dynamics and stochastic processes coexist [19]. In order to model the stochastic process, we define a stochastic jump as a process stochastically resulting in an increment of damage fraction $\Delta p = 1/N$. The Hamming distance between the two successive states is $H = 1$, i.e., they are neighboring states. The most important consequence of the stochastic jump is to trigger a mode transition from GS to EIC . This is what can actually occur in the sensitive zone [12, 19].

Macroscopically, this sensitivity can be described by transition probability $\psi_N(p, \sigma_0)$. This is the probability of a stochastic jump induced mode transition from GS to EIC, for GS states with damage fraction p_0 under nominal stress σ_0 (or critical ligament L_c). In other words, Ψ_N is the probability of a stochastic jump induced transition from a mode with a globally stable final state to a mode which eventually evolves to catastrophe. $\psi_N(p, \sigma_0)$ is the averaging of μ defined in Equation (18) over all the GS states with damage fraction p_0 for given σ_0. One can deduce an approximate relationship between transition probability $\psi_N(p, \sigma_0)$ and failure probability $\Phi_N(p, \sigma_0)$ as follows:

$$\psi_N(p_0, \sigma_0) = \frac{\Phi_N\left(p_0 + \frac{1}{N}, \sigma_0\right) - \Phi_N(p_0, \sigma_0)}{1 - \Phi_N(p_0, \sigma_0)}. \tag{19}$$

For long period case, for example $N > 30$, Equation (19) becomes quite accurate. The size effect of ψ_N has the same scaling law as Φ_N.

The multi-scale phenomena with disordered smaller scales are universal in nature. In thermodynamic equilibrium, behaviors on a larger scale can be derived from the statistical average of phenomena on smaller scales. However, the trans-scale sensitivity indicates that a simple statistical average may no longer be sufficient to describe the nonlinear non-equilibrium evolution of a disordered system. A minor difference in smaller scales may be strongly enhanced during nonlinear evolution and this appears to have a major effect on a larger scale. Such events are closely related to the sensitive zone in phase space. For material failure, the trans-scale sensitivity switches the problem 'to be or not to be', so it is extremely important.

8. Conclusion

Material failure is a complex phenomenon owing to its intrinsic features, such as multi-scales, disorder and nonlinear evolution. The complexity manifests itself as an evolution-induced catastrophe, sample-specific behavior and trans-scale sensitivity. In order to investigate these aspects, we examined a simple model – a periodic chain. The slice sampling method has been developed to analyze ensemble evolution and to calculate failure probability and mode transition probability.

The results demonstrate that the periodic chain can reproduce some fundamental complicated behavior of material failure. This behavior is universal in systems with multi-scales, disorder and nonlinear evolution. It is noticeable that there is a transitional region in space of macroscopic variables, e.g. the damage fraction p_0 and the nominal stress σ_0. The statistical descriptions, such as the binary failure probability and the transition probability, are essential in the phenomenon. Furthermore, the size effects of the transitional region approximately obey scaling laws. It is also noticeable that there is a sensitive zone in phase space which plays a fundamental role in the sample-specific behavior of material failure, the trans-scale sensitivity and the evolution-induced catastrophe. This indicates that one has to go deep into the sensitive zone if intending to understand the complexity observed in material failure.

Acknowledgment

This work is supported by the National Fundamental Research Project 'Nonlinear Science' and National Natural Science Foundation of China (No. 19732060, 19572072 and 19577102).

References

1. Sahimi, M. and Arbabi, S., 'Mechanics of disordered solid. III. Fracture properties', *Physical Review B* **47**, 1993, 713–722.
2. de Arcangelis, L., Redner, S., and Herrmann, H. J., 'A random fuse model for breaking processed', *Journal of Physics (Paris)* **46**, 1985, 585–590.
3. Meakin, P., 'Models for material failure and deformation', *Science* **252**, 1991, 226–234.
4. Bai, Y. L., Lu, C.S., Ke, F. J., and Xia, M. F., 'Evolution induced catastrophe', *Physics Letters A* **185**, 1994, 196–200.
5. Xia, M. F., Song, Z. Q., Xu, J. B., Zhao, K. H., and Bai, Y. L., 'Sample-specific behavior in failure models of disordered media', *Communication in Theoretical Physics* **25**, 1996, 49–54.
6. Liang, N., Liu, Q., Li, J., and Song, H., 'A chains net-work model simulating meso mechanical behavior and micro damage evolution of in situ reinforced ceramics, in *Advanced in Engineering Plasticity & Its Applications*, T. Abe and T. Tsuta (eds.) Pergamon, Amsterdam, 1996, pp. 141–146.

7. Ibnabdeljalil, M. and Curtin, M. A., 'Strength and reliability of fiber-reinforced composites: Localized load-sharing and associated size effects', *International Journal of Solids Structures* **34**, 1997, 2649–2668.
8. Harlow, D. G. and Phoenix, S. L., 'Probability distribution for the strength of composite materials I: two-level bonds', *International Journal of Fracture* **17**, 1981, 347–372.
9. Hemmer, R. C. and Hause, H., 'The distribution of simultaneous fiber failures in fiber bundles', *ASME Journal of Applied Mechanics* **59**, 1992, 909–914.
10. Durbury, P. M. and Leath, P. L., 'Failure probability and average strength of disordered systems', *Physical Review Letters* **72**, 1994, 2805–2908.
11. Xia, M. F., Bai, Y. L., and Ke, F. J., 'Statistical description of pattern evolution in damage-fracture', *Science in China (A)* **37**, 1994, 331–340.
12. Xia, M. F., Ke, F. J., Bai, J., and Bai, Y. L., 'Threshold diversity and trans-scale sensitivity in a nonlinear evolution model', *Physics Letters A* **236**, 1997, 60–64.
13. Herrmann, H. J. and Roux, S., *Statistical Models for the Fracture of Disordered Media*, North-Holland, Amsterdam, 1990.
14. Bai, Y. L., Ke, F. J., and Xia, M. F., 'Deterministically stochastic behavior and sensitivity to initial configuration in damage fracture', *Science Bulletin* **39**, 1994, 892–895 [in Chinese].
15. Ke, F. J., Fang, X., Xia, M. F., Zhao, D. W., and Bai, Y. L., 'Contingent sensitivity to configuration in a nonlinear evolution system', *Progress in Natural Science* **8**, 1998, 170–173.
16. Xia, M. F., Wu, W. M., Zhang, C. F., and Zhao, K. H., 'Characteristics of the basins of attraction in neutral network dynamics', in *Proceedings of Beijing International Workshop on Neural Networks*, K. H. Zhao, C. F. Zhang, and Z. X. Zhu (eds.), World Scientific, Singapore, 1989, pp. 116–123.
17. Knott, J. F., *Fundamentals of Fracture Mechanics*, Butterworths, London, 1973.
18. Xing, X. S., 'The foundation of nonequilibrium statistical fracture mechanics', *Advances in Mechanics* **21**, 1991, 153–168 [in Chinese].
19. Xia, M. F., Bai, Y. L., and Ke, F. J., 'A stochastic jump and deterministic dynamics model of impact failure evolution with rate effect', *Theoretical and Applied Fracture Mechanics* **24**, 1996, 189–196.